Available online at www.sciencedirect.com
ScienceDirect
Journal of the European Ceramic Society 28 (2008) 1191–1196
www.elsevier.com/locate/jeurceramsoc

Influence of zirconia addition on the microstructure of $K_{0.5}Na_{0.5}NbO_3$ ceramics

Barbara Malic *, Janez Bernard, Andreja Bencan, Marija Kosec

Jožef Stefan Institute, Jamova 39, 1000 Ljubljana, Slovenia

Received 12 April 2007; received in revised form 30 October 2007; accepted 2 November 2007
Available online 3 January 2008

Abstract

We prepared $(K_{0.5}Na_{0.5})NbO_3$ (KNN) ceramics with the addition of 1 mass% ZrO_2 with the aim to hinder the exaggerated grain growth encountered in KNN. Both KNN and KNN-ZrO_2 ceramics sintered at 1115 °C and 1125 °C, respectively, had relative density exceeding 95%. KNN had a bimodal microstructure, with a population of fine grains of a few 100 nm and the large grains of about 20 μm, while the microstructure of KNN-ZrO_2 was fine and uniform, with the median grain size of 0.3 μm and the largest grains of about 1.3 μm. We attribute the refinement of the microstructure to the matrix grain-growth inhibition by ZrO_2 addition. The influence of ZrO_2 is twofold: sub-100 nm sized ZrO_2 particles, located at the KNN grain junctions hinder the matrix grain growth. Additionally, the enrichment of the boundary regions of the matrix grains with Zr relative to the grain interiors, confirmed by TEM/EDXS analysis, is also a probable reason for the decreased mobility of the grain boundaries. The dielectric permittivity and losses, measured at 10 kHZ, and piezo d_{33} constant of KNN-ZrO_2 are 905, 0.04 and 100 pC/N, respectively.

Keywords: Microstructure-final; Piezoelectric properties; Niobates; ZrO_2; Lead-free; (K,Na)NbO_3

1. Introduction

The research on lead-free piezoelectric ceramics as a possible alternative to widely exploited lead-based complex perovskites such as $Pb(Zr,Ti)O_3$ (PZT) and $Pb(Mg_{0.33}Nb_{0.67})O_3$-$PbTiO_3$ (PMN-PT)-based materials has been stimulated by the increased consciousness for health and environment protection. The group of materials based on $K_{0.5}Na_{0.5}NbO_3$ (KNN) has been intensively studied especially since the discovery of the compositions modified with lithium and tantalum with piezoelectric properties comparable to those of commercial PZT materials.[1] The KNN itself has got a moderate piezoelectric response, i.e. d_{33} between 80 pC/N and 100 pC/N after normal sintering[2,3] and almost 150 pC/N in the case of spark-plasma sintering.[4] Due to its biocompatibility it could be used for medical applications.[5]

The difficulties related to undoped KNN are sintering and control of microstructure and/or stoichiometry. The temperature range of atmosphere-sintering of KNN is narrow and close to its melting point at 1140 °C, spanning from 1100 °C to 1120 °C.[3,6,7] Our previous study of the microstructure of KNN ceramics sintered at 1100 °C with 94.9% of theoretical density revealed a bimodal distribution of grain sizes with fine micrometer sized grains and a fraction of large grains ranging up to a few 10 μm. Sodium-deficient niobium-rich second-phase inclusions were also determined in the microstructure.[6] A bimodal grain size distribution was observed by Zhen and Li[8] in Li-doped and Li/Ta-codoped KNN and attributed to volatilization of sodium oxide. The same authors further reported a core-shell structure of coarse grains of KNN and Li/Ta codoped KNN. The core consisted of oriented nanosized subgrains and the shell of larger subgrains. They proposed that the growth of the coarse grains was mediated by volatilization of alkalines (sodium oxide) and formation of liquid phase.[9] Bimodal microstructure of KNN was also reported by Du et al.[7]

KNN ceramics have got adequate piezoelectric and material properties for ultrasonic medical transducers.[10] To improve sensitivity and consequently resolution, the transducer should operate at higher frequencies, therefore the thickness of the piezoelectric element, a ceramic disk, should be low.[11] Ceramics with a non-uniform microstructure are difficult to cut to small dimensions and also fine grinding and polishing of thin disks may be a problem. Therefore the aim of our work was

* Corresponding author.
E-mail address: Barbara.malic@ijs.si (B. Malic).

0955-2219/$ – see front matter © 2007 Elsevier Ltd. All rights reserved.
doi:10.1016/j.jeurceramsoc.2007.11.004

to prepare dense fine-grained KNN ceramics with atmosphere sintering. Fine-grained microstructure should also yield higher mechanical strength and consequently it would allow easier surface finishing. Although it has been demonstrated that the grain growth of KNN can be decreased by the addition of different aliovalent dopants, as for example Sr or Mg,[12,3], or Li/Ta,[8] the idea in this work was to add second-phase inclusions which would limit grain growth of the matrix phase.

Zirconia inclusions effectively inhibit grain growth of alumina matrix, with the prerequisite that all four-grain junctions of the matrix grains should be filled with zirconia particles, which is at ≥5 vol.%, but even a lower amount decreased the ratio of the largest to the average grain size.[13] The addition of ZrO_2 in the amount of 1 mass% (or 1.3 vol.%) to $(Pb_{0.94}Sr_{0.06})(Zr_{0.52}Ti_{0.48})O_3$ ceramics caused a decrease of the matrix grain size, increased flexural strength and yielded piezoelectric properties only slightly lower than of PZT itself. Increasing the addition of ZrO_2 up to 8 vol.% improved the strength but deteriorated the piezo-response.[14] According to our knowledge, there are no data on (K,Na)NbO_3-ZrO_2 phase relations. However, as both ionic radius and coordination of Nb^{5+} and Zr^{4+} are similar,[15] chemical interaction between the two phases should be considered as well.

In this work we added 1 mass% of zirconia particles to the synthesized KNN powder. We investigated the influence of zirconia addition on the density, phase composition, microstructure, dielectric permittivity and piezoelectric d_{33} coefficient of the ceramics.

2. Experimental

$K_{0.5}Na_{0.5}NbO_3$ (KNN) was synthesized from the binary perovskite compounds. $KNbO_3$ and $NaNbO_3$ were prepared by milling niobium oxide (99.9%, Sigma–Aldrich) and potassium tartrate ($K_2C_4H_4O_6{\cdot}0.5H_2O$, >99.5%, Fluka) or sodium tartrate ($Na_2C_4H_4O_6{\cdot}2H_2O$, >99.5%, Riedel de Haën), respectively, in an attrition mill with yttria-stabilized zirconia (YSZ) balls for 4 h in acetone. The powder mixtures were heated at 700 °C in case of $KNbO_3$ or 650 °C for 4 h in case of $NaNbO_3$ and milled for 4 h. The equimolar mixture of $KNbO_3$ and $NaNbO_3$ was wet-milled for 1 h, calcined at 950 °C for 4 h and milled again for 4 h.

Zirconia powder (99.96%, Tosoh) in the amount of 1 mass% was added to the synthesized KNN powder. The blend was homogenized in a planetary mill in acetone for 15 min. This mixture is further denoted as KNN-ZrO_2.

The KNN and KNN-ZrO_2 powders were uniaxially pressed with 300 MPa and sintered at 1115 °C and 1125 °C for 2 h in air, respectively.

The samples for microstructural analysis were mounted in epoxy, grinded and polished using standard metallographic techniques. The polished samples were thermally etched at 50 °C below the sintering temperature for 30 min. Plan view TEM samples were prepared by mechanical thinning, dimpling and ion milling using 3.8 keV argon ions.

Density was calculated from mass and dimensions of ceramic pellets.

The microstructures were analyzed by scanning electron microscope JEOL 5800 (SEM) and an analytical electron microscope JEM 2010F (TEM). Both microscopes were equipped with a LINK ISIS 300 energy-dispersive X-ray spectrometer (EDXS). Due to strong overlapping of the Zr(L) and Nb(L) lines in the case of SEM-EDXS (20 kV), analytical electron microscopy was used. Using 200 kV accelerating voltage and Si–Li detector the Na Kα, K Kα, Nb Lα and Zr Kα spectral lines were used for the quantitative TEM-EDXS analysis. Single crystals of $KNbO_3$ and $NaNbO_3$ were used as reference materials to improve the accuracy of the quantitative SEM/EDXS analysis, especially when analyzing sodium.[6,16]

Thermally etched samples were analyzed by a field emission SEM (FE-SEM, Supra 35 VP, Carl Zeiss). The digitalized microstructure was processed with the Image Tool software[17] to obtain the areas of more than 200 grains. The grain size was expressed as Feret's diameter. The roundness factor R was calculated as the ratio $4\pi A/P^2$, where A is grain area and P its perimeter.[18]

For electrical characterization gold electrodes were sputtered on the polished disks with 6.5 mm diameter and 0.6 mm thickness. Capacitance and tan δ were measured at 10 kHz (Hewlett Packard 4192 LF Impedance Analyzer). The samples were poled at 100 °C with 2 kV/mm and 6.5 kV/mm for KNN and KNN-ZrO_2, respectively. The piezo d_{33} constant was determined by a Berlincourt piezo d_{33} meter (Take Control).

3. Results and discussion

The geometrical density of KNN-ZrO_2 ceramics is 4.30 g cm^{-3}, which is comparable to 4.31 g cm^{-3} (95.5% of theoretical density) obtained for pure KNN.

SEM micrographs of the fracture, polished and thermally etched surfaces of the two materials are collected in Fig. 1. The fracture surface of KNN reveals a non-uniform microstructure with regions of both trans- and intra-granular fracture (Fig. 1a). We can distinguish grains, ranging from about a micrometer up to a few 10 μm. The SEM-BEI image of the polished surface shows the dark-grey matrix phase with pores, which are non-uniform in size and in distribution (Fig. 1b). The content of porosity estimated from the polished microstructure is much larger than the value obtained from the geometrical calculus of density, which is 5%. We assume that in the process of grinding and polishing the sample experienced pullouts which could explain the presence of regularly shaped voids in the microstructure. We observed some light-grey second-phase inclusions, marked with an arrow, but their area was too small for an exact analysis.

The thermally etched surface reveals a strongly bimodal microstructure, consisting of cube-shaped grains ranging from a few 100 nm to about a micrometer, and a population of large grains of sizes of up to a few 10 μm (Fig. 1c). Note that the sample is over-etched, but with lower etching times the boundaries of the fine grains could not be discerned.

The fracture surface of KNN-ZrO_2 is predominantly transgranular (Fig. 1d). The polished microstructure contains uniformly distributed sub-micron pores and some light-grey

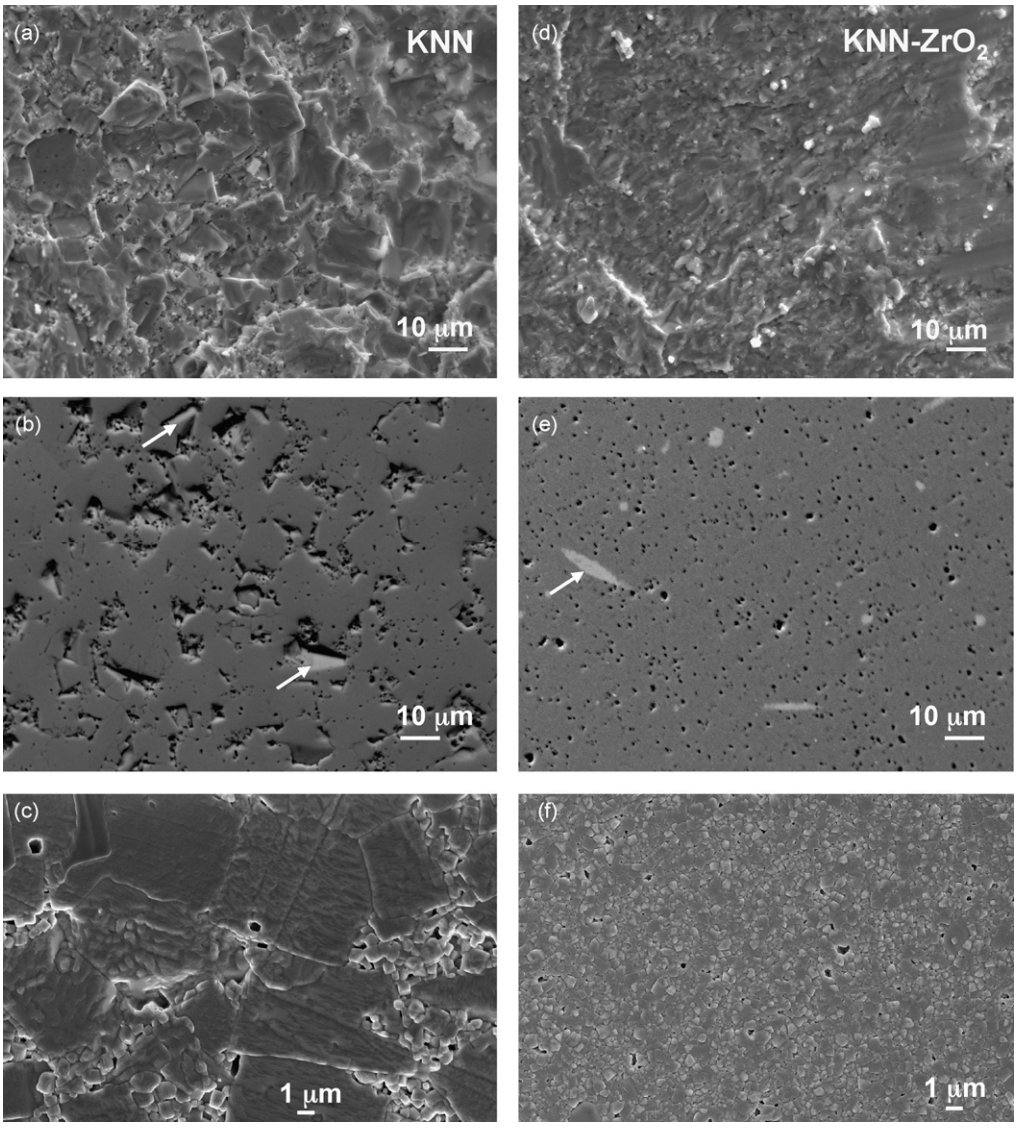

Fig. 1. Fracture surfaces (a and d), polished (b and e) and thermally etched microstructures (c and f) of KNN and KNN-ZrO_2 ceramics. (a and b), (d and e): SEM-BEI; (c and f): FE-SEM micrographs.

second-phase inclusions (Fig. 1e). EDXS analysis of the matrix phase yielded the composition corresponding to 10.24 at.% Na, 10.23 at.% K and 21.07 at.% Nb. The Na/K and the (Na + K)/Nb ratios were 1 and 0.97, the latter slightly lower than the theoretical value of 1. The second-phase inclusions contained a lower amount of Na in relation to K and to Nb, namely the Na/K and the (Na + K)/Nb ratios were 0.74 and 0.85, respectively (Table 1). A sodium-deficient and niobium-rich secondary phase with the Na/K and (Na + K)/Nb ratios equal to 0.30 and 0.60 was determined by SEM/EDXS in the microstructure of KNN, sintered at 1100 °C for 24 h.[6] The deficiency of sodium in KNN-based ceramics was also observed by Zhen and Li.[8] Zr could not be detected by EDXS which we attribute to its low content, homogeneous distribution in the matrix phase, and to overlapping of the characteristic Nb Lα and Zr Lα spectral lines.

Table 1
Elemental composition of the matrix and secondary phase in KNN-ZrO_2 ceramics determined by SEM/EDXS analysis

	At.%[a]			Na/K	(Na + K)/Nb
	Na	K	Nb		
Nominal composition	10	10	20	1	1
Matrix	10.24 ± 0.50	10.23 ± 0.0.05	21.07 ± 0.05	1.00	0.97
Second phase	7.85 ± 0.64	10.59 ± 0.20	21,65 ± 0.02	0.74	0.85

[a] The at.% of Na, K and Nb were normalized assuming ABO_3 stoichiometry. The results are the average of three analyses at different locations on the sample.

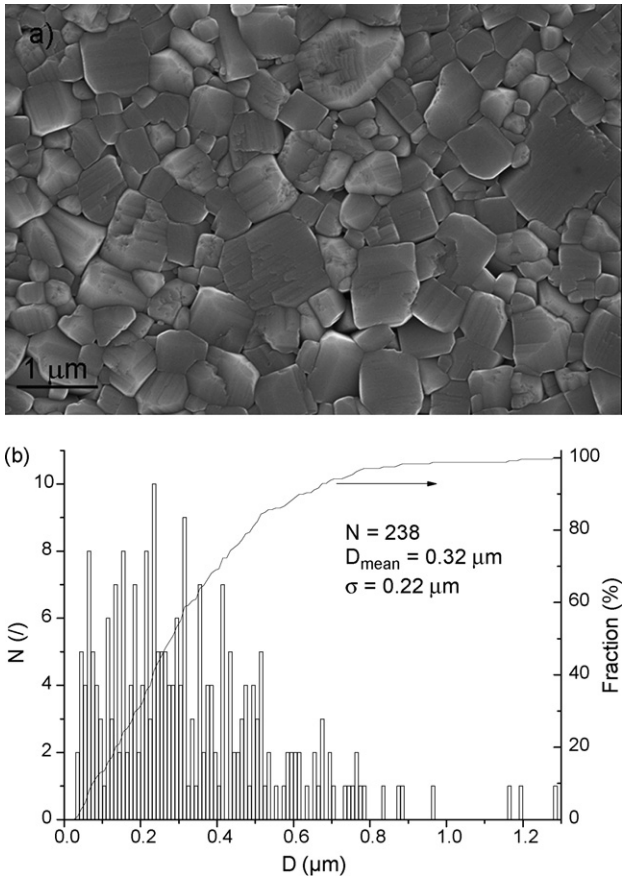

Fig. 2. Thermally etched microstructure (a) and grain size distribution (b) of KNN-ZrO_2 ceramic. N: number of grains, D: Feret's diameter.

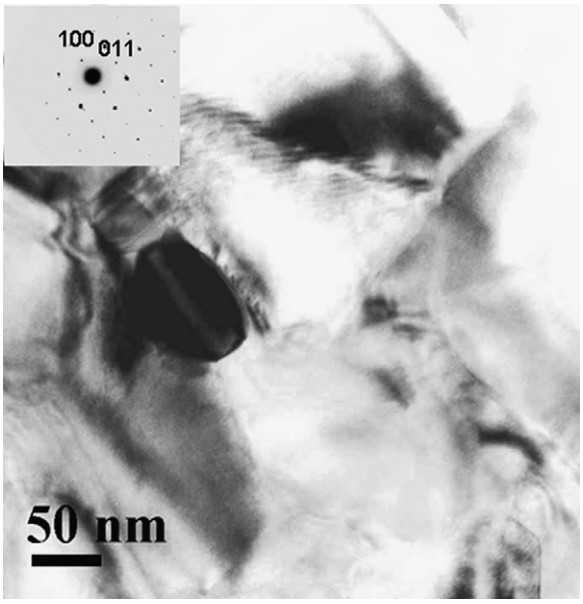

Fig. 4. Bright field TEM image of a ZrO_2 grain in a [0,1,−1] zone axis located at the junction of KNN matrix grains. Inset: selected area electron diffraction (SEAD) pattern of the ZrO_2 grain.

The thermally etched surface of KNN-ZrO_2 ceramics consists of uniform sub-micron grains (Fig. 1f) and is in strong contrast to the bimodal microstructure of KNN (Fig. 1c). The predominantly cuboidal shape of the grains is clearly discernible at a higher magnification (Fig. 2a). Note that the matrix and ZrO_2 grains cannot be distinguished. The grain size distribution is unimodal, with the mean grain size equal to 0.32 ± 0.22 μm. The largest measured grains do not exceed 1.3 μm. The roundness factor *R*, which describes the deviation from a perfectly circular shape, is 0.67 (Fig. 2b).

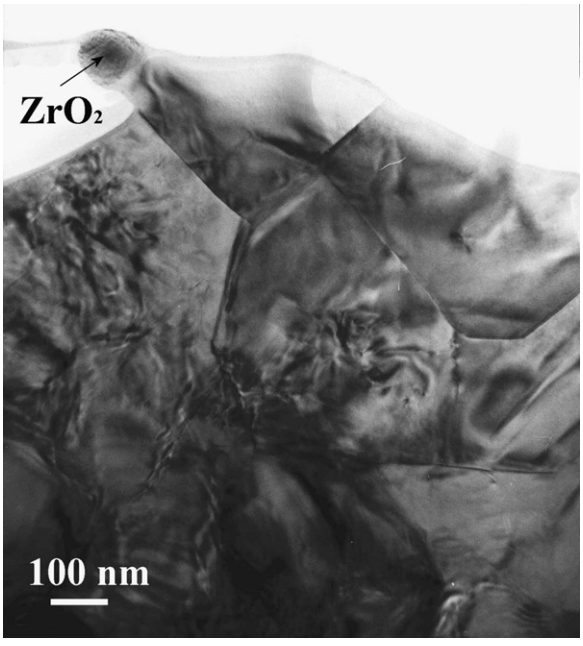

Fig. 3. Bright field TEM image of the perovskite grains with flat grain boundaries and well discernible ferroelectric domains in KNN-ZrO_2 ceramic.

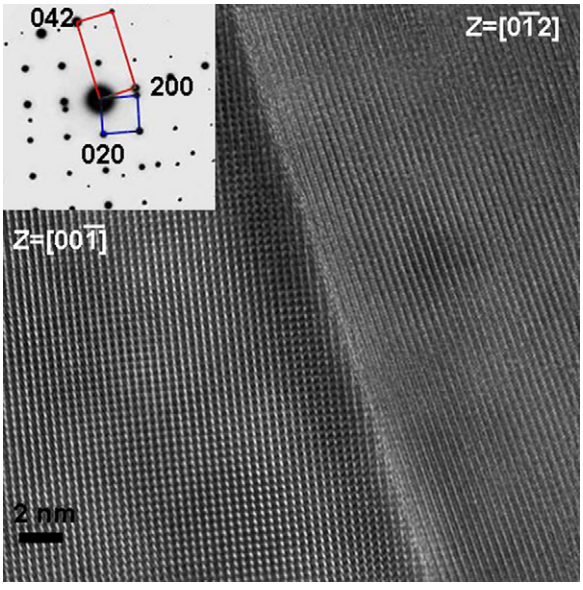

Fig. 5. High-resolution TEM image of a boundary between two perovskite grains. SAED pattern performed on the boundary was indexed with monoclinic KNN unit cell (PDF: 77-0038). It shows reflections of KNN grains in [0,0,−1] and in [0,−1,2] zone axis.

Table 2
Dielectric permittivity and losses measured at 10 kHz and piezoelectric d_{33} constant measured with Berlincourt meter of KNN and KNN-ZrO_2 ceramics

	ε	$\tan\delta$	d_{33} (pC/N)
KNN	580	0.08	80
KNN-ZrO_2	905	0.04	100

A detailed study of the microstructure of the KNN-ZrO_2 ceramics was further performed by transmission electron microscopy. The morphology of cube-shaped grains with flat grain boundaries and ferroelectric domains is discernible in Fig. 3. This observation is in agreement with an earlier study of KNN ceramics sintered at 1100 °C[6] and TEM study of 0.95 $K_{0.5}Na_{0.5}NbO_3$, −0.05 $BaTiO_3$ sintered at 1060 °C.[19] The ZrO_2 inclusions of around 50 nm in size were found at the junctions of the matrix grains (Figs. 3 and 4). The SAED confirmed the monoclinic structure of ZrO_2.[20]

A high-resolution TEM analysis of the matrix revealed clean grain boundaries, with no segregation of second phases between the grains (Fig. 5). We could not detect the sodium-deficient secondary phase inclusions observed by SEM. It is possible that they were etched in the process of sample preparation.

We further investigated a possible interaction between the two phases. The analysis of four matrix grains consistently yielded a higher content of Zr in the 5 nm region close to the grain boundary in comparison to the grain interior (Fig. 6). The enrichment of the grain boundary region in zirconium can be explained by the diffusion of zirconium in the perovskite lattice. Having in mind that the ionic radius and coordination chemistry of Zr ions are similar to Nb, we can expect a limited solid solubility of Zr in $K_{0.5}Na_{0.5}NbO_3$ with Zr^{4+} occupying the Nb^{5+} sites in the perovskite lattice. Consequently vacancies should form in the O-sublattice.

Such defect structure in the boundary region of the grain could impede KNN grain growth. It has been shown for $BaTiO_3$ that the non-uniform distribution of the dopant within the grain interior, and with a higher concentration of the dopant in the boundary region, limits the grain growth. Examples include $BaTiO_3$ doped with Nb,[21] Bi/Nb,[22] Ce,[23] La,[24] and Mg.[25]

We further measured the dielectric and piezoelectric properties of KNN and KNN-ZrO_2 ceramics. The dielectric permittivity, losses and piezo d_{33} constant of KNN are 580, 0.08 and 80 pC/N, in agreement with reported data.[2,3] The respective values for KNN-ZrO_2 are 905, 0.04 and 100 pC/N (Table 2). Note also that the KNN-ZrO_2 sample could be poled with a three times higher electric field than the KNN. We can connect higher dielectric permittivity and piezoelectric d_{33} coefficient of KNN-ZrO_2 ceramics with the observed changes in microstructure in comparison to KNN. Matrix characterization of the KNN-ZrO_2 ceramics is being carried out from impedance measurements at resonance on three-sample geometries[26] and will be published separately.

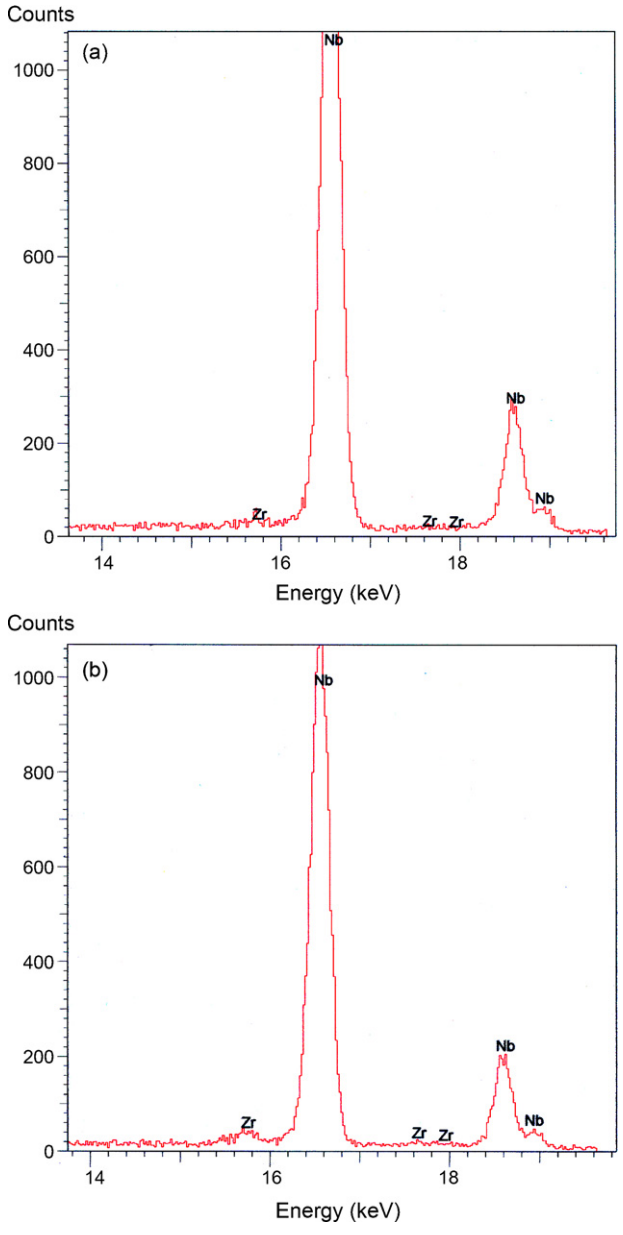

Fig. 6. TEM/EDXS spectra of the KNN grain interior (a) and of the region close to the KNN grain boundary (b). The spot size was 5 nm.

4. Summary

We have shown that the addition of a small amount of ZrO_2 particles effectively hinders the grain growth of $K_{0.5}Na_{0.5}NbO_3$ ceramics during sintering in air. We attribute the refinement of the microstructure to two processes. The zirconia particles located at the matrix grain junctions decrease the mobility of the matrix grain boundaries, however in our case the amount of ZrO_2 is too low to fill the majority of grain junctions. By TEM/EDXS we detected enrichment of KNN grain boundary regions relative to the grain interior which we attributed to a limited solubility of Zr in the perovskite lattice. We connect this defect structure of the grain boundary regions with the hindrance of the matrix grain growth. The dielectric permittivity, losses and piezo d_{33} constant of KNN-ZrO_2 are 905, 0.04 and 100 pC/N.

Acknowledgements

The authors wish to acknowledge the financial support of Slovenian Research Agency (P2-105) and of the EC in the Network of Excellence MIND (NMP3-CT2005-515757). We would like to thank Ms. Jena Cilenšek for support in the experimental work and Elena Daniela Ion, M.Sc. for FE-SEM analysis of selected samples. Dr. Marjan Bele is acknowledged for allowing access to FE-SEM at the National Institute of Chemistry, Ljubljana, Slovenia.

References

1. Saito, Y., Takao, H., Tani, T., Nonoyama, T., Takatori, K., Homma, T., Nagaya, T. and Nakamura, M., Lead-free piezoceramics. *Nature*, 2004, **432**, 84–87.
2. Jaffe, B., Cook Jr., W. R. and Jaffe, H., *Piezoelectric Ceramics*. Academic Press, London, 1971, pp. 185–212.
3. Malic, B., Bernard, J., Holc, J., Jenko, D. and Kosec, M., Alkaline earth doping in (K,Na)NbO_3 based piezoceramics. *J. Eur. Ceram. Soc.*, 2005, **25**, 2707–2710.
4. Zhang, B.-P., Li, J.-F., Wang, K. and Zhang, H., Compositional dependence of piezoelectric properties in $Na_xK_{1-x}NbO_3$ lead-free ceramics prepared by spark plasma sintering. *J. Am. Ceram. Soc.*, 2006, **89**(2), 706–709.
5. Nilsson, K., Lidman, J., Ljungström, K., and Kjellman, C., Biocompatible material for implants. WO Patent 99/54266, 1999.
6. Jenko, D., Bencan, A., Malic, B., Holc, J. and Kosec, M., Electron microscopy studies of potassium sodium niobate ceramics. *Microsc. Microanal.*, 2005, **11**, 572–580.
7. Du, H., Li, Z., Tang, F., Qu, S., Pei, Z. and Zhou, W., Preparation and piezoelectric properties of $K_{0,5}Na_{0,5}NbO_3$ lead-free piezoelectric ceramics with pressure-less sintering. *Mater. Sci. Eng.*, 2006, **B 131**, 83–87.
8. Zhen, Y. and Li, J.-F., Normal sintering of (K,Na)NbO_3-based ceramics: influence of sintering temperature on densification, microstructure, and electrical properties. *J. Am. Ceram. Soc.*, 2006, **89**(12), 3669–3675.
9. Zhen, Y. and Li J. -F., Abnormal grain growth and new core-shell structure in (K,Na)NbO3-based lead-free piezoceramics. *J. Am. Ceram. Soc.*, 2007, doi:10.1111/j.1551-2916.2007.01977.x.
10. Tran-Huu-Hue, L. P., Feuillard, G., Loyau, V., Ringgaard, E. and Lethiecq, M., Non-linear behaviour of piezoelectric materials with graded electromechanical properties. In *Proceedings WCU 2003*, 2003, pp. 543–546.
11. Lethiecq, M., Levassort, F. and Tran-Huu-Hue, L.-P., Ultrasonic transducers for high resolution imaging: from piezoelectric structures to medical diagnostics. *Informacije MIDEM*, 2006, **35**, 177–186.
12. Kosec, M. and Kolar, D., On activated sintering and electrical properties of $NaKNbO_3$. *Mater. Res. Bull.*, 1975, **10**, 335–340.
13. Lange, F. F. and Hirlinger, M. M., Hindrance of grain growth in $A1_20_3$ by $Zr0_2$ inclusions. *J. Am. Ceram. Soc.*, 1984, **67**(3), 164–168.
14. Malic, B., Kosec, M. and Kosmac, T., Mechanical and electric properties of PZT-ZrO_2 composites. *Ferroelectrics*, 1992, **129**, 147–155.
15. Shannon, R. D., Revised effective ionic radii and systematic studies of interatomic distances in halides and chalcohalides. *Acta Cryst.*, 1976, **A3**, 751–767.
16. Samardzija, Z., Bernik, S., Marinenko, R. B., Malic, B. and Ceh, M., An EPMA study on $KNbO_3$ and $NaNbO_3$ single crystals—potential reference materials for quantitative microanalysis. *Microchim. Acta*, 2004, **145**, 203–208.
17. UTHSCSA *Image Tool Version 3.00*, 2002.
18. Chinn, R. E., *Ceramography: Preparation and Analysis of Ceramic Microstructures*. John Wiley & Sons, New York, 2002, pp. 145–157.
19. Lee, H. J., Ryu, H., Bae, M.-S. and Cho, Y. K., Transmission electron microscopy microstructure of 0.95 $Na_{0.5}K_{0.5}NbO_3$ −0.05$BaTiO_3$ ceramics. *J. Am. Ceram. Soc.*, 2006, **89**(11), 3529–3532.
20. JCPDS-International Centre for Powder Diffraction data PDF 88-2390.
21. Buessem, W. R. and Kahn, M., Effects of grain growth on the distribution of Nb in $BaTiO_3$ ceramics. *J. Am. Ceram. Soc.*, 1971, **54**(9), 458–461.
22. Hennings, D. and Rosenstein, G., Temperature-stable dielectrics based on chemically inhomogeneous $BaTiO_3$. *J. Am. Ceram. Soc.*, 1984, **67**(4), 249–254.
23. Park, Y. and Kim, H. G., The microstructure analysis of cerium-modified barium titanate having core-shell structured grains. *Ceram. Int.*, 1997, **23**, 329–336.
24. Urek, S., Drofenik, M. and Makovec, D., Sintering and properties of highly donor-doped barium titanate ceramics. *J. Mater. Sci.*, 2000, **35**, 895–901.
25. Park, J. S. and Han, Y. H., Effects of MgO coatings on microstructure and dielectric properties of $BaTiO_3$. *J. Eur. Ceram. Soc.*, 2007, **27**, 1077–1082.
26. Pardo, L., Algueró, M. and Brebøl, K., A non-standard shear resonator for the matrix characterization of piezoceramics and its validation study by finite element analysis. *J. Phys. D: Appl. Phys.*, 2007, **40**, 2162–2169.